MODELLING OF AERODYNAMIC FORCES AND HEAT TRANSFER FOR ORBITAL DECAY AND RE-ENTRY CALCULATIONS

Dr. Ing. G. Koppenwallner
Dipl.Ing. D. Johannsmeier

HTG
Max Planck Straße 1
3411 Lindau Harz

ABSTRACT

In order to improve orbital decay and re-entry calculations of satellites an appropriate aerodynamic modelling is necessary. The aerodynamic data along the trajectory can be provided either in numerical tables generated by large computer codes or by anylytical formulae.
The last way requires a simplified description of the vehicle shape and aerodynamic flow models for free molecular flow , rarefied flow and hypersonic continuum flow.

1. INTRODUCTION.

We may generally distinguish between orbital- and reentry aerodynamics.

Important points for orbital aerodynamics are:

- Space objects may vary considerably in size and shape e.g.
  Large satellites and space stations (L > 10 m)
  Small debris particles ($L > 10^{-3}$ m)
- Shape not designed by aerodynamic considerations.
- Satellite attitude relative to velocity vector is usually not constant .
  e.g Spin stabilized satellites
  Tumbling satellites
- Due to size variation ballistic coefficient can vary in an extremely large range.

Important points for entry aerodynamics of satellites are:

- Entry altitude $h_{bmax.}$ can vary in a large range.
  e.g H = 100 km for small debry particle
  H = 40 km for heavy satellite (NPS)
  Fig. 1 explaines this.

- Entry mostly uncontrolled, therefore
  angle of attack
  dynamic oscillations unknown

Analytic aerodynamic tools, which can be implemented in trajectory and entry codes shall therefore consider these points.

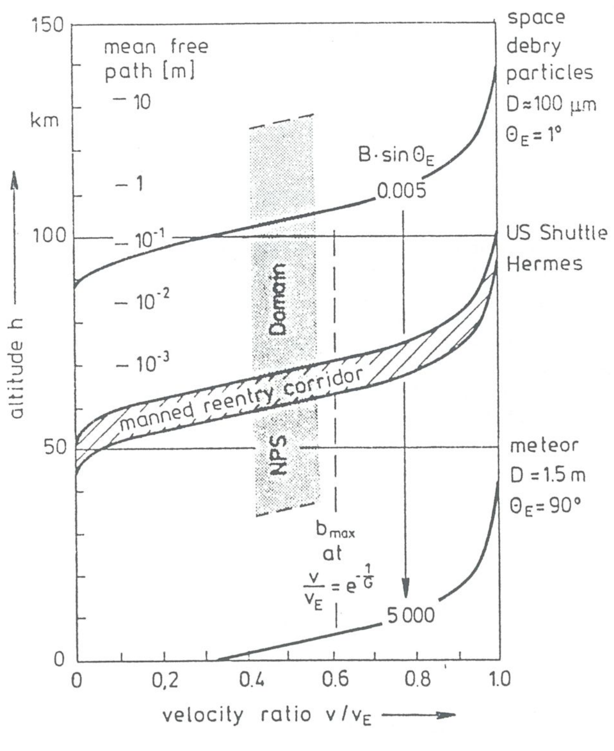

Fig. 1 The spread of reentry altitudes for Space objects with different ballistic coefficient B .
$B = m/(c_D A)$, θ_E Entry angle

2. THE FLOW REGIMES

We distinguish three flow regimes (see Fig. 2)

Free molecular flow	$Kn > 5$
Rarefied transitional flow	$5 > Kn > 0.001$ or $Ma / \sqrt{Re} > .1$
Hyperonic Continuum Flow	$Kn < 0.001$ or $Ma / \sqrt{Re} < .1$

It shall be remembered that the above flow regime boundaries are shape dependent.

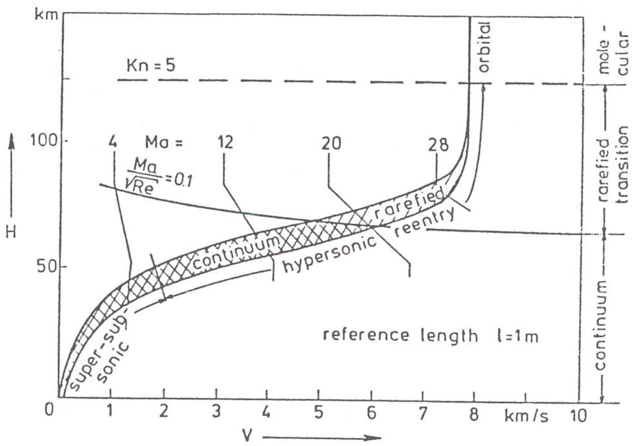

Fig. 2 Reentry flow regimes

3. THE SHAPE DESCRIPTION.

Complex shapes can be described by
finite surface elements, e.g Boettcher (Ref.1).
or
shape elements.

We use the shape element method in order to compose a complex configuration (Ref.2).
Fig 3. explains this method on the example of KOSMOS 1870.

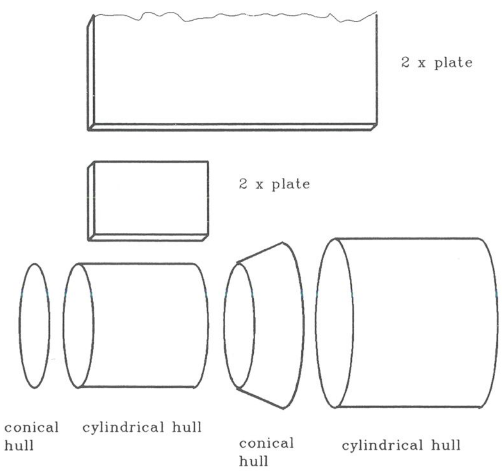

Fig. 3 The division of KOSMOS 1870 into shape elements

4. THE FREE MOLECULAR FLOW MODEL.

The following stepwise approach is used in order to obtain analytical formulae.

1. From the exact free molecular formulation, which is only valid for convex surface elements, we deduce approximate expressions
for local surface pressure
local skin friction

2. We distingish between slender and blunt surface element aerodynamics, which depends on the inclination α' of the surface element against the flow. The following criteria is used (Ref.3). Surface element dS local inclination α'
slender $\alpha' < \mu$, with $\mu = 1/ S$
blunt $\alpha' > \mu$, with $\mu = 1/ S$

3. We use the Pike-method (Ref.4) to determine the integral aerodynamic forces (drag, lift) for the various shape elements.
Every shape element is characterized by typical shape coefficients, which result from Integrals over the wetted surface.

$$c_D = \int_s c'_x ds \qquad = \sum N_p D_p \quad , p = 0\text{-}3$$

$$c_L = \int_s c'_y \operatorname{cosec} \delta \, (\bar{n}\cdot\bar{l}) \, ds \quad = \sum T_p L_p \, .$$

Explanations:

N_p and T_p : local aerodynamic coefficients

D_p and L_p : shape integrals e.g

$D_p = (-1)^p \int_s (\bar{v} \cdot \bar{n})^p \, dS$, e.g

D_0 = surface area, D_1 flow projected area of shape

4. As example of derived aerodynamic formula may serve a spherical cap. For drag and lift coefficient we obtain the following set of equations:

Analytical formula for drag - and lift coefficient of a spherical cap in free molecular flow.

Boundary : $\alpha < (\frac{\pi}{2} - \vartheta)$ with ϑ = opening angle

$$c_D = \left(2\sigma_t + \frac{2-\sigma_n}{S_\infty^2}\right)\cos\alpha +$$

$$\left(\sigma_n \frac{\sqrt{\pi}}{S_\infty}\sqrt{\frac{T_w}{T_\infty}}\right)\left[\left(c_{S1}+\frac{1}{6}\right)+\left(\frac{1}{2}-c_{S1}\right)\cos 2\alpha\right] +$$

$$\left(2(2-\sigma_n)-2\sigma_t\right)\frac{1}{8}\left[3\left(c_{S2}+1\right)\cos\alpha + \left(5c_{S2}-3\right)\cos 3\alpha\right]$$

$$C_L = \left(\frac{2-\sigma_n}{S_\infty^2}\right)(-\sin\alpha) +$$

$$\left(\sigma_n \frac{\sqrt{\pi}}{S_\infty}\sqrt{\frac{T_w}{T_\infty}}\right)\left(C_{S1}-\frac{1}{2}\right)\sin 2\alpha +$$

$$\left(2(2-\sigma_n)-2\sigma_t\right)\frac{1}{8}\left[-\left(C_{S2}+1\right)\sin\alpha-\left(5C_{S2}-3\right)\sin 3\alpha\right]$$

The equations contain two shape dependend coefficients C_{S1} and C_{S2}.

$$C_{S1} = \frac{1}{2}\cdot\frac{1}{1+\cos\vartheta} \quad ; \quad C_{S2} = 1-\frac{1}{2}\sin^2\vartheta$$

Each equation consists of three terms, which have some special physical relevance.
Term 1 gives for diffus reflection ($\sigma_n = \sigma_t = 1.$) the contribution of the incident flux to the aerodynamic coefficients.
Term 2 shows the influence of the wall temperature on drag and lift.
Term 3 vanishes for diffus molecular reflection .

5. TYPICAL RESULTS .

The following two figures show results for typical shape elements.

Slender shape: cylindrical hull, Fig. 4
Blunt shape: spherical cap , Fig. 5

We compare with these two cases the analytical solutions with the exact forces determined by a surface element method of DLR (Ref.1).

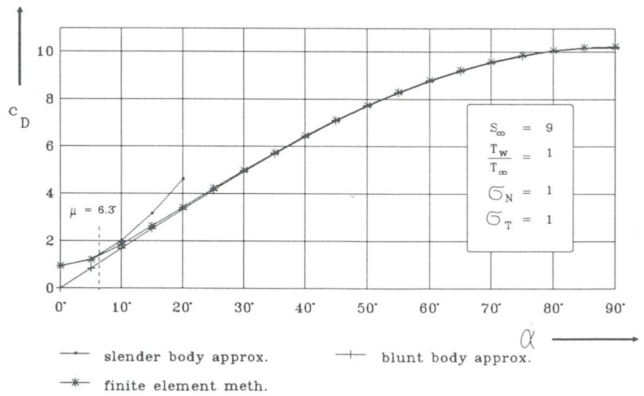

Fig. 4 Drag coefficient of a cylindrical hull (length/diameter l/d = 3.7)

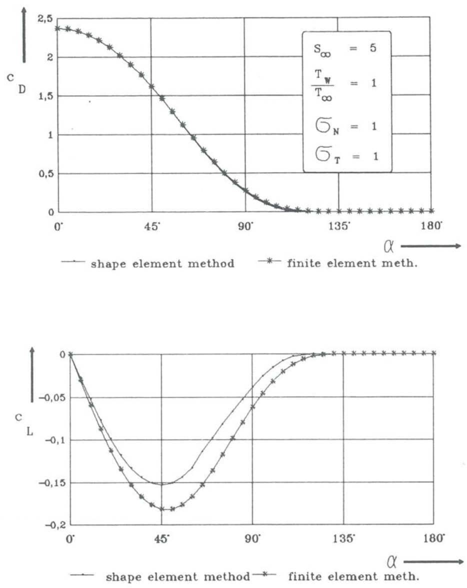

Fig. 5 Drag and lift coefficient of a spherical cap (diameter / nose radius $d/r_N = 1$)

The treatment of concave shapes.

In order to treat concave shapes we adopt a control surface method.The concave shape is surrounded by a control surface, which must be passed by all molecules hitting the body. This approximation is however exact only for the limiting speed ratio case $S_\infty=\infty$. Fig.6 explains the method.

As application we selected Salyut 7, which has concave elements between its solar panels.
Fig. 7 shows the drag coefficient as function of rotation angle, and the integrated mean coefficient over one complete rotation.
Calculations as shown in this figure have been used to predict the Salyut 7 decay.

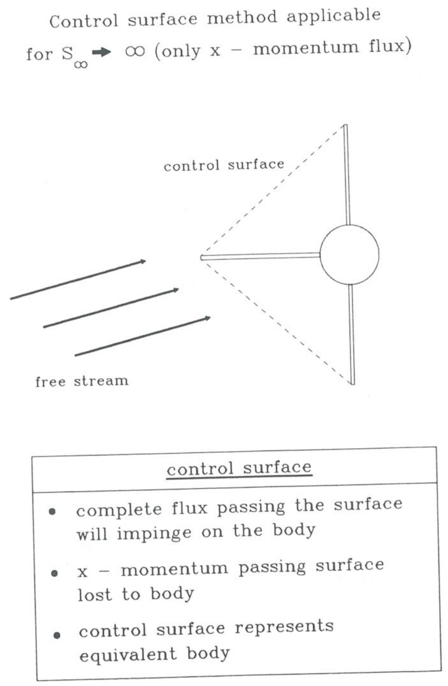

Fig. 6 The aproximate treatment of concave shapes.

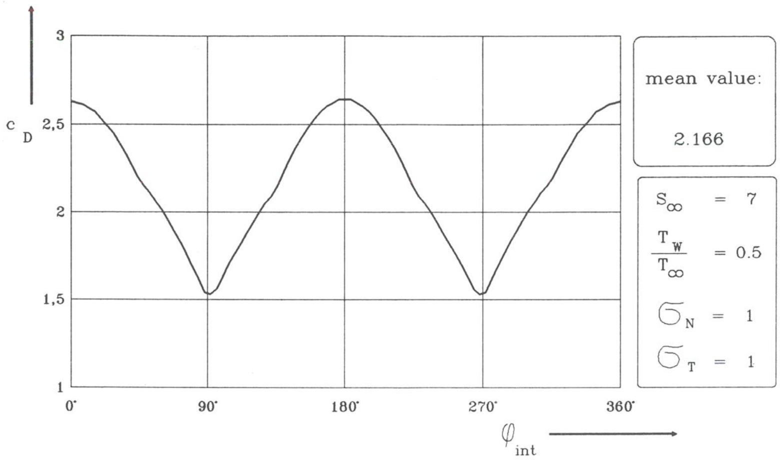

Fig. 7 Drag coefficient of Salyut7/Kosmos 1686

6. THE REENTRY FLOW MODELLING.

During reentry flow the space craft passes

from	free molecular
through	rarefied transition
to	hypersonic continuum flow.

There exist however some exeptions from this rule. A small space debry particle may be decelerated completely in free molecular flow. In this case $c_{DFreemol.}$ is needed as function of speed ratio S.

Fig. 8 shows the typical behaviour of the drag coefficient c_D and the heat transfer Stanton number ST as function of Knudsen number during reentry (Ref. 5).

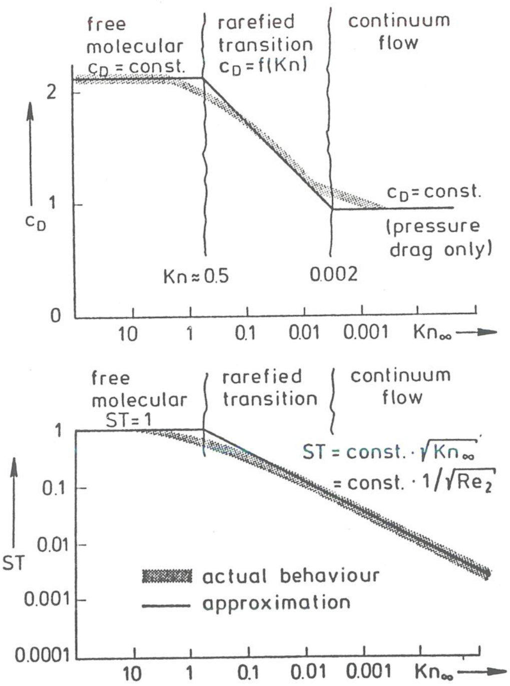

Fig.8 Behaviour of aerodynamic coefficients and approximation in the various flow regimes.

6.1 The continuum flow model.

The modified Newtonian theory is used in the Pike formulation.
We obtain analytical drag and lift formulae for a wide variety of shape elements.
For shapes having two symmetry planes through the main axis we derived e.g the following formulae:

$\alpha = 0$: $c_D = k_N C_S$ with

k_N = Newton Factor

C_S = Shape Factor

$\alpha \neq 0$: (validity wetted area constant)

$$c_D = \frac{k_N}{2} \cos\alpha \left(2\ C_S - (5\ C_S - 3\ )\sin^2(\alpha)\right)$$

$$c_L = \frac{k_N}{2} \sin\alpha \left(2\ (1 - 2\ C_S\ ) - (5\ C_S - 3\ )\sin^2(\alpha)\right)$$

The free molecular formulae shown in section 4 degenerate to Newtonian formulae by inserting proper values for S_∞, T_W/T_1, σ_N, σ_T, namely
$S_\infty = \infty$; $T_W/T_1 = 0$; $\sigma_N = 1$; $\sigma_T = 0$.

For a spherical cap the free molecular shape coefficient C_{S2} equals the Newtonian shape coefficient C_S.

Fig. 9 shows the universal Newtonian drag and lift functions for angles of attack between $\alpha = 0 - 90°$. The shape coefficient C_S , which determines the drag at $\alpha = 0°$, serves as parameter. The functions are however only valid under the condition that with increasing α the wetted surface is the same as at $\alpha = 0°$.With increasing geometric body bluntness - i.e increasing C_S- the Newtonian shadowing is however shifted to higher angles of attack.

We observe that depending on C_S the lift slope at $\alpha = 0°$ may be positive or negative.

C_S	body shape	lift slope at $\alpha = 0°$
< 0.5	slender	positive
> 0.5	blunt	negative

This demonstrates that blunt entry bodies like the capsules will experience a negative lift for a positive defined angle of attack.

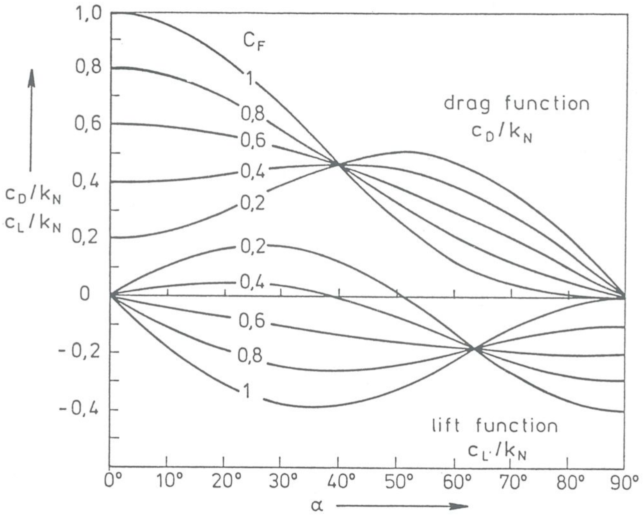

Fig. 9 The Newtonian drag and lift function for bodies with two symetry planes.

6.2 The bridging between free molecular and continuum flow.

There exist several approaches to close the gap between the two flow regimes.

$$\text{Free molecular} \xrightarrow[\textit{methods}]{\textit{bridging}} \text{continuum flow.}$$

Typical approaches for bridging are :

> Local bridging with finite surface element method, which is used in USSR (Ref. 6 and DLR (Ref. 7).
> Bridging of integral coefficients as developed by L. Potter , USA , (Ref. 8).
> Bridging of shape element description (our approach).

The last two methods allow to derive analytical formulae for trajectory programms.
The basic bridging relations must however be derived from experimental data.
As example of our approach may serve again the spherical cap.
For this family of shape elements we derived bridging relations for the normalized drag coefficient c_D as shown in Fig. 10.

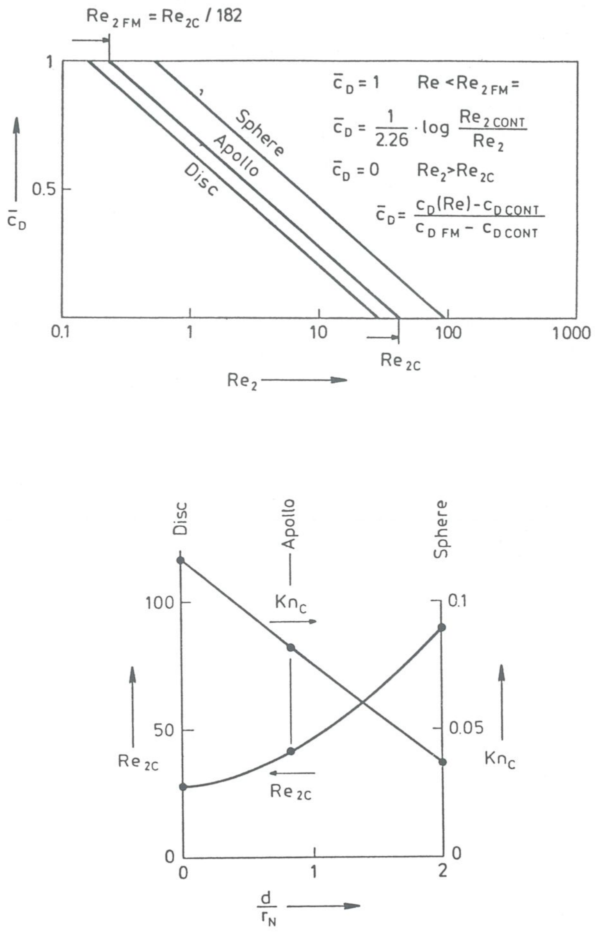

Fig. 10 The bridging relations for spherical caps. Note Reynolds number Re_2 can be related to Knudsen number Kn.

7. CONCLUSION

In free molecular aerodynamics the largest uncertainties are connected with

> Complex, concave shape modelling.
> Unknown spacecraft attitude
> Gas- Surface Interaction law.
> Non- Diffuse reflection will be of major importance on concave shapes with multiple wall collisions.

For entry of small particles the free molecular aerodynamic formulation must cover the whole range of speed ratios between $20 > S_\infty > 0$.

Transitional flow prediction with bridging methods is still in a state of developement.

Complex numerical schemes ,like DSMC methods, are too time consuming for application in trajectory calculations.

Aerodynamic methods for trajectory calculations are mostly used by experts with limited aerodynamic background, therefore the method design must consider this user environment.

8. REFERENCES

1. Boettcher R.D. 1979 , The calculation of convex body aerodynamics in free molecular flow using a plane element surface approximation, DFVLR IB 251-79 A 13

2. Koppenwallner G. Johannsmeier D. 1990 , Analytical and Numerical Formulation of Lift and Drag of Satellites in Free Molecular Flow. HTG Rep. 90-3

13. Koppenwallner G. 1988, Aerodynamik von Satelliten , Handbuch der Raumflugtechnik, Hanser Verlag, München , pp 440 -482.

4. Pike J. 1979, Forces on Convex Bodies in Free Molecular Flow, AIAA Journal,Vol..13, pp 1454-1459.

5. Koppenwallner G. 1989, Rarefied Gas Dynamics. in Hypersonics Volume I, Defining Hypersonic Environment, Birkhäuser , Boston.

6.Kotov V.M Lychin E.N.Reshin A.G. 1982 An approximate Method of aerodynamic calculation of complex shape bodies in a transition region. Rarefied Gas DynamicsVol.1, Plenum Press, New York.

7. Boettcher R.D. 1991 Applicability of Bridging Methods to Hypersonic Rarefied Flow Aerodynamics. Proc. of 1th European Symposium on Aerothermodynamics for Space Vehicles.

8. Potter J.L. 1988 Procedure for Estimating of the Aerodynamics of Three-Dimensional Bodies in Transitional Flow. in Rarefied Gas Dynamics, Vol 118 of Progress in Astronautics and Aeronautics , AIAA, USA.